

## EXPERIMENTAL AND NUMERICAL DYNAMIC ANALYSIS OF A CRACKED BEAM

**Luciano Rizzatti**

SIFCO S/A, Av São Paulo, 361 – CEP 13202-610, Jundiaí, SP  
lrizzatti@sifco.com.br

**José Maria Campos dos Santos**

Universidade Estadual de Campinas, UNICAMP/FEM/DMC, Cx.P. 6122, 13083-970, Campinas, SP  
zema@fem.unicamp.br

**Abstract.** *This investigation describes the implementation of a beam finite element with a crack in central region for any crack length. The element simulates the dynamic behavior of a rectangular cross section beam with three degrees of freedom per node including shear effect and plastic zone at the crack tip. The element was implemented in MATLAB environment and the results were compared with ones available in the literature. Simulated results are also compared with the experimental modal analysis performed in the steel rectangular cross section beams containing different crack depths. The results shown a good agreement between numerical and experimental models, which represents an interesting mechanism to be used for structural failure prediction due the presence of cracks.*

**Keywords:** *cracked beam, finite element, plastic zone, fracture mechanics.*

### 1. Introduction

Vibration investigation of damaged structure is an approach for fault diagnosis. Vibration diagnosis, as a non-destructive technique, has becomes of greater importance. In the last years, many works were performed in order to develop a non-destructive inspection based on vibration theory, which allow cracks identifying and evaluating from natural frequency, vibration mode, and dynamic response signal variations. Methods that allow evaluating a structure in service have a great interest to different industrial applications, like mobility industry, nuclear and hydroelectric power station and large equipments of production in general.

The main point of this study is that a mechanical component or a structure that contains a crack has their stiffness reduced, which reflects as a dynamic behavior change.

A crack on an elastic structural element introduces considerable local flexibility due to the strain energy concentration in the vicinity of the crack tip under load. In this study it was used the Finite Element Method (FEM) to simulate the dynamic behavior change in vicinity of crack tip. It was developed a beam element that simulates the reduction of stiffness according to crack properties.

In the last decades many papers have been published in this direction. Dimaragonas and Papadopoulos (1983) presented a cracked finite element with a crack that contains a single opening mode due bending load. Three years later, Dimaragonas and Papadopoulos (1986) expanded this theory to consider all the possible crack opening modes (tensile, bending and torsion). Qian, Gu and Jiang (1990) developed a cracked rectangular cross section beam finite element, obtained through stress intensity factor integration. This theory was used by Sekhar and Prabhu (1994) in floating stress at rotor bearing system containing a crack. Sekhar and Balaji Prasad (1997) studied the effect of a slant crack in rotor with a circular cross section. In 1998, Kisa, Brandon and Topcu develop a cracked finite element based in substructure approximation. Krawczuk, Zak and Ostachowics (2000) studied a finite element based on elasto-plastic fracture mechanics.

This paper presents a two nodes cracked beam finite element with rectangular cross section, three degrees of freedom per node, and a crack position in the middle of element length. It includes the effects of shear effort and crack tip plasticity.

### 2. Cracked beam finite element

#### 2.1. Stiffness matrix

The cracked beam finite element stiffness matrix is composed by two parts: the first one is an uncracked beam finite element matrix based on Timoshenko beam analytical model; the second is a local cracked beam finite element stiffness matrix obtained through additional displacements due the crack, based on fracture mechanics theory. The cracked beam stiffness matrix is obtained by summing both parts. The finite element configuration is shown in Fig. 1.

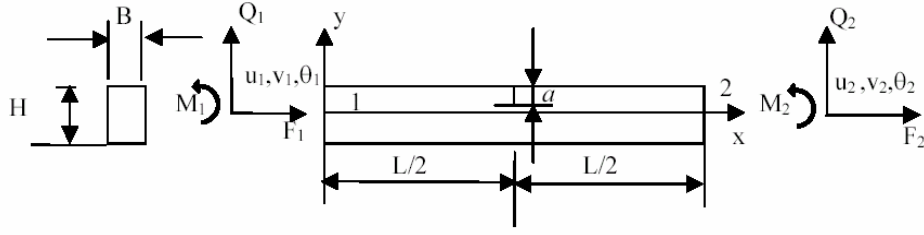


Figure 1. Schematic model of implemented element

From the fracture mechanics theory the additional displacement  $u_i$  due to the depth crack  $a$  in the direction  $i$  can be written as (Tada, Paris and Irwin, 2000):

$$u_i = \frac{\partial}{\partial P_i} \int_A \mathcal{G} dA \quad (1)$$

where  $\mathcal{G}$  is the Strain Energy Density Function (SEDF) and  $P_i$  is the corresponding load. The complete equation of SEDF is given by (Dimarogonas and Papadopoulos, 1983):

$$\mathcal{G} = \frac{1}{E'} \left[ \left( \sum_{j=1}^6 K_{Ij} \right)^2 + \left( \sum_{j=1}^6 K_{IIj} \right)^2 + (1+\nu) \left( \sum_{j=1}^6 K_{IIIj} \right)^2 \right] \quad (2)$$

where  $E' = E$  or  $E' = E/(1-\nu^2)$  for plane stress and plane strain respectively,  $E$  is the Young's modulus,  $\nu$  is the Poisson ratio and  $K_{ij}$  are the crack Stress Intensity Factors (SIF) for the opening mode (*I, II, III*) and for the applied load ( $j=1, 2, \dots, 6$ ). For the presented model two opening modes (*I* and *II*) and three different loads (axial, bending and shear) were used, then the specific SEDF is given by (Rizzatti, 2004):

$$\mathcal{G} = \frac{1-\nu^2}{E} \left\{ (K_I(F) + K_I(M))^2 + K_{II}^2(Q) \right\} \quad (3)$$

According to Dimarogonas and Papadopoulos (1983), the local flexibility due the crack per unit width is:

$$c_{ij} = \frac{\partial u_i}{\partial P_j} \quad (4)$$

or the flexibility can be expressed using the equation of SEDF:

$$c_{ij} = \frac{\partial}{\partial P_i} \left( \frac{\partial}{\partial P_j} \int_A \mathcal{G} dA \right) \quad (5)$$

The values of SIF in Equation (2) are well known from the literature (Tada, Paris and Irwin, 2000) for a strip of unit thickness with a transverse crack. Since the energy density is a scalar and assuming that crack depth is variable and the stress intensity factor is given by the elementary strip it is allowed to integrate along the crack tip. It is known that this approximation yields acceptable results to engineering accuracy. The expressions for stress intensity factor to the modes I and II and applied loads (axial, bending and shear loads) considered in the model are:

$$K_I(F) = \frac{F}{BH} \sqrt{\pi a} f_1\left(\frac{a}{H}\right) \quad (6)$$

$$K_I(M) = \frac{6M}{BH^2} \sqrt{\pi a} f_2\left(\frac{a}{H}\right) \quad (7)$$

$$K_{II}(Q) = \frac{\kappa Q}{BH} \sqrt{\pi a} f_3\left(\frac{a}{H}\right) \quad (8)$$

where  $f_1, f_2$ , and  $f_3$  are called as correction functions and are detailed as:

$$f_1\left(\frac{a}{H}\right) = \sqrt{\frac{2H}{\pi a} \tan\left(\frac{\pi a}{2H}\right)} \frac{\left[0,752 + 2,02\left(\frac{a}{H}\right) + 0,37\left(1 - \sin\left(\frac{\pi a}{2H}\right)\right)^3\right]}{\cos\left(\frac{\pi a}{2H}\right)} \quad (9)$$

$$f_2\left(\frac{a}{H}\right) = \sqrt{\frac{2H}{\pi a} \tan\left(\frac{\pi a}{2H}\right)} \frac{\left[0,923 + 0,199\left(1 - \sin\left(\frac{\pi a}{2H}\right)\right)^4\right]}{\cos\left(\frac{\pi a}{2H}\right)} \quad (10)$$

$$f_3\left(\frac{a}{H}\right) = \frac{\left[1,122 - 0,561\left(\frac{a}{H}\right) + 0,085\left(\frac{a}{H}\right)^2 + 0,180\left(\frac{a}{H}\right)^3\right]}{\sqrt{1 - \frac{a}{H}}} \quad (11)$$

By substituting equations (6), (7), (8) and (3) in (5) the expression for flexibility coefficients can be given by:

$$c_{ij} = \frac{\partial u_i}{\partial P_j} = \frac{\partial^2}{\partial P_i \partial P_j} \int_A \left[ \frac{1 - \nu^2}{E} \left\{ (K_I(F) + K_I(M))^2 + K_{II}^2(Q) \right\} \right] dA \quad (12)$$

Then, the local cracked beam finite element flexibility matrix can be written as,

$$C_c = \begin{bmatrix} c_{11} & 0 & c_{13} \\ 0 & c_{22} & 0 \\ c_{31} & 0 & c_{33} \end{bmatrix} \quad (13)$$

and the uncracked beam finite element flexibility matrix is given by:

$$C_0 = \begin{bmatrix} \frac{L}{EA} & 0 & 0 \\ 0 & \frac{1}{12} \frac{L^3 \left(4 + \frac{12\kappa EI}{GAL^2}\right)}{EI} & \frac{1}{2} \frac{L^2}{EI} \\ 0 & \frac{1}{2} \frac{L^2}{EI} & \frac{L}{EI} \end{bmatrix}$$

The local cracked beam finite element flexibility matrix is added to the uncracked beam finite element flexibility matrix, to obtain the cracked beam finite element flexibility matrix as shown as:

$$C = C_0 + C_c \quad (14)$$

and the cracked beam finite element stiffness matrix will be its inverse,

$$K_c = C^{-1} \quad (15)$$

## 2.2. Elasto-plastic local flexibility of a cracked beam

From the elasto-plastic fracture mechanics a plastic zone is developed closed to the crack tip always that stresses exceed the material yield strength. Then the flexibility of such structures increases more than is observed in the case of purely elastic materials. As applied by Krawczuk, Zak and Ostachowics (2000) the effect of flexibility increasing due to the

crack tip yielding was modeled as an hypothetical extension of the crack tip,  $r_p$ , as shown in Fig. 2. The plastic zone radius around the crack tip  $r_p$ , to the crack fracture mode I (opening mode) can be calculated from the relationship:

$$r_p \approx \frac{1}{6\pi} \left( \frac{K_I}{\sigma_{yp}} \right)^2 \quad (16)$$

where  $K_I$  is the elastic stress intensity factor and  $\sigma_{yp}$  the material yield strength.

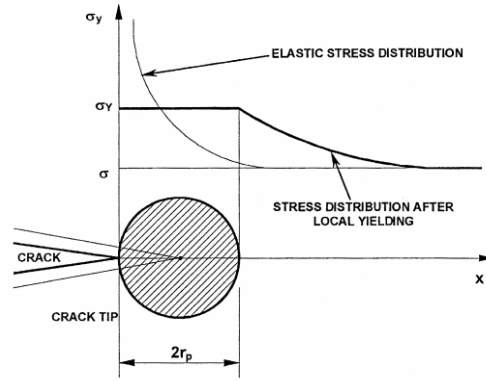


Figure 2. Crack tip plastic zone (Krawczuk, Zak and Ostachowics, 2000).

Considering the plastic zone around the crack, the stress intensity factor  $K_{IP}$  can be expressed as:

$$K_{IP} = f_i \sigma \sqrt{\pi(a + r_p)} \quad (17)$$

where  $a$  is the crack length,  $f_i$  is a correction function which takes into account the body and crack geometry, and  $\sigma$  is the applied nominal stress.

Substituting equation (16) into (17) and applying in equations (6) and (7), leads to the new expression of the stress intensity factor considering the effects of plastic zone:

$$K_{IP}(F) = \frac{F}{BH} \sqrt{\pi a} f_1 \sqrt{1 + \frac{1}{6} f_1^2 \left( \frac{\sigma}{\sigma_{yp}} \right)^2} \quad (18)$$

$$K_{IP}(M) = \frac{6M}{BH^2} \sqrt{\pi a} f_2 \sqrt{1 + \frac{1}{6} f_2^2 \left( \frac{\sigma}{\sigma_{yp}} \right)^2} \quad (19)$$

Then, the equations (18) and (19) can be substituted into equation (12) to obtain the local flexibility coefficients including plastic zone effect.

### 3. Numerical results and element convergence

The cracked beam finite element was implemented in MEFLAB (Pavanello, 1995), a finite element code developed in MATLAB environment. Due its similarities with the implemented element and also to contain experimental results, the same example of Qian, Gu & Jiang (1990) was performed to verify the implemented cracked finite element. Qian's model consists of a single cracked finite element with length  $L$ , a crack in the middle of element length, two degrees of freedom per node with bending, but without plasticity and shear effects. The element configuration is shown in Fig. 3a:

To compare the results from both elements the same mesh as described in Quian's paper was performed in the implemented element, which is composed of 5 elements and 6 nodes. Also, same dimensions and constraints were applied to simulate a cantilever beam, where  $z$  is the crack position related to constrained beam end,  $L_v=200.0$  mm is the beam length,  $a$  is crack length,  $z/L_v$  is relative position,  $H=7.8$  mm and  $B=1.0$  mm are cross section height and width, respectively. The used material is steel with the following properties: Young's modulus  $E=210$ Gpa; Poisson coefficient  $\nu=0.28$ ; and density  $\rho=7860$  kg/m<sup>3</sup>. Figure 3b shows the main dimensions and mesh to the beam example.

Since natural frequencies depends on the crack position, crack size and beam geometric dimensions, the comparison

among results from simulated implemented element, Qian's simulated element and Qian's experimental are presented using plots of relative natural frequencies values ( $f_{ti}/f_{ni}$ ) versus relative crack depth ( $a/H$ ). Where  $f_{ti}$  and  $f_{ni}$  are the natural frequencies with and without crack for the mode  $i$ , respectively. Figures 4 – 9 show the results for the 3 first bending natural frequencies and relative position,  $z/L_v = 0.20, 0.30, 0.40, 0.55, 0.60$ , and  $0.70$ . For all cases analyzed the results of implemented element shows a good agreement with ones from Qian's simulated and experimental.

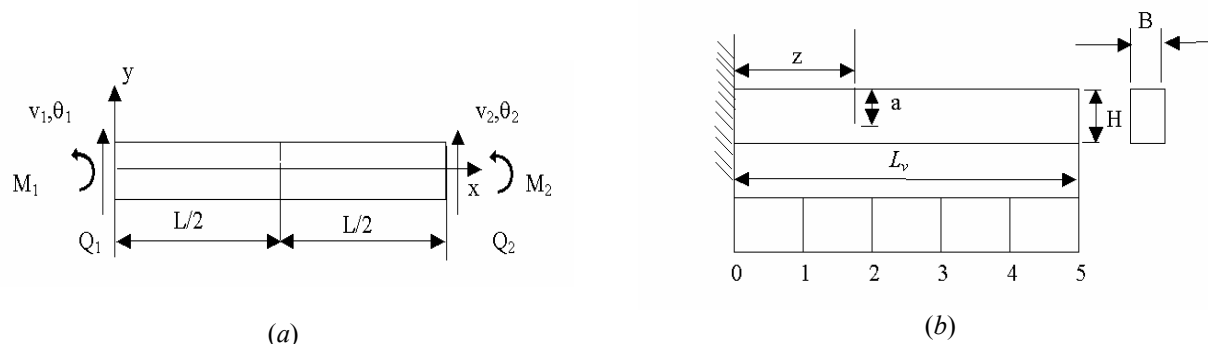


Figure 3. Qian, Gu & Jiang (1990) model: (a) finite element and (b) beam example.

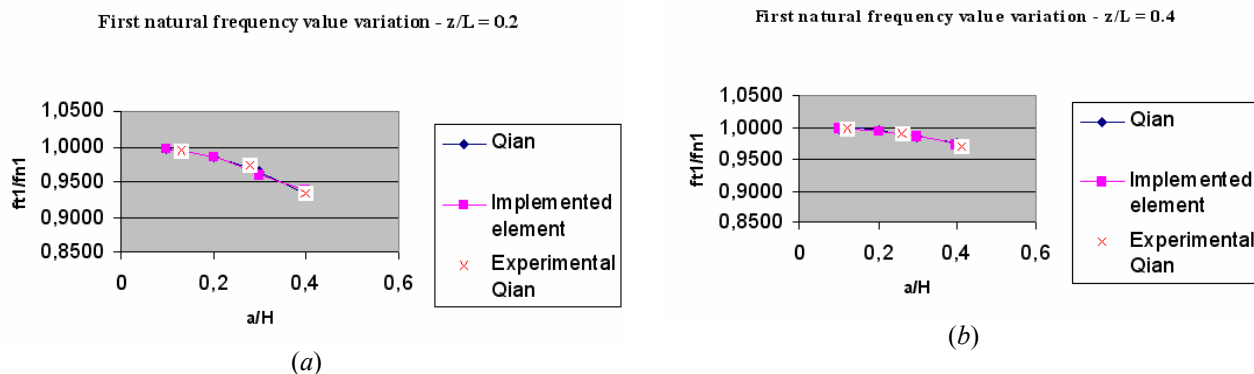


Figure 4. First bending natural frequency and  $z/L_v = 0.2$  and  $0.4$ .

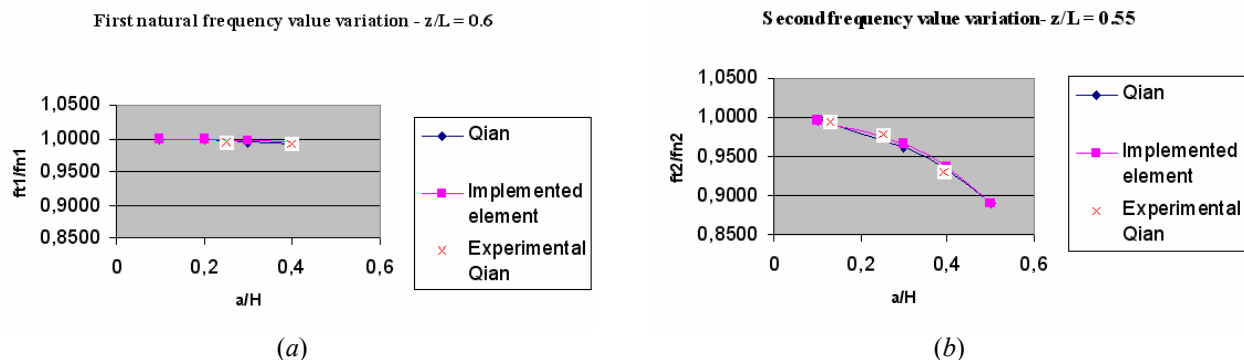


Figure 5. First and second bending natural frequency for  $z/L_v = 0.6$  and  $0.55$ .

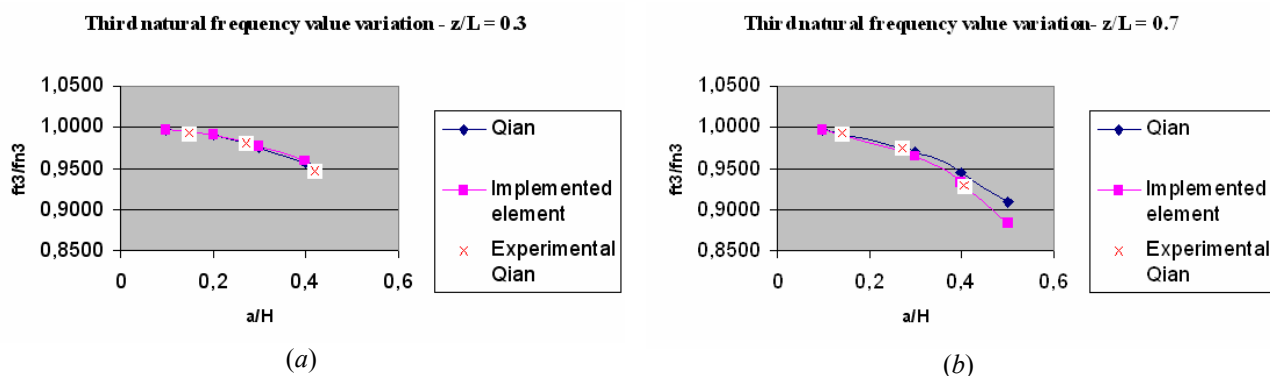


Figure 6. Third bending natural frequency and  $z/L_v = 0.3$  and  $0.7$

The convergence of the implemented finite element was evaluated using the same beam example, but with a free-free boundary condition and for different mesh sizes. Numerical modal analysis using a mesh size beam with 1, 3, 9, 19 and 39 elements and cracked elements with  $a/H = 0.2$  and  $0.5$  were simulated. Figure 10 shows the results for the 2 first natural frequencies versus the number of elements. For both cases it could be seen that by using a mesh with 9 or more elements the natural frequencies variations will be inferior to 1.5%. Although the results to third natural frequency are not presented here, its behavior is similar to the others.

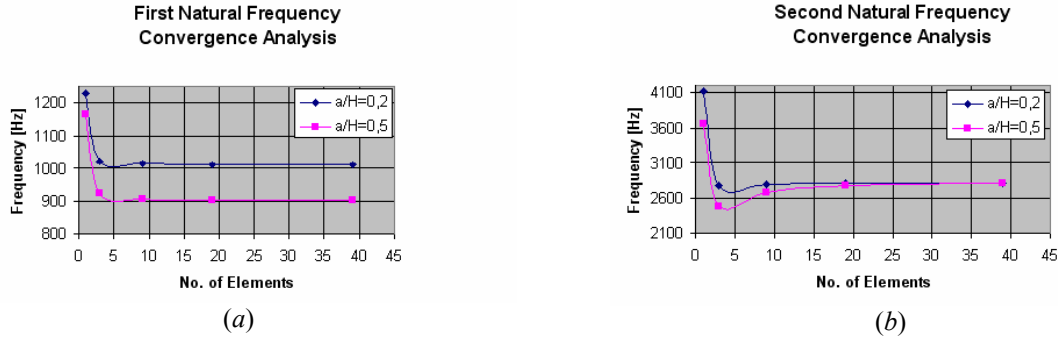


Figure 7. First and second natural frequency element convergence plot.

#### 4. Experimental results

In order to validate the simulated results from the implemented element, experimental modal analysis using four same dimension beams with different crack length and one without crack were performed in free-free boundary conditions.

The beams are made in SAE 1018 steel with rectangular cross section ( $H = 30.0$  mm and  $B = 15.0$  mm) and length  $L = 400.0$  mm (Fig. 11a). A 1.0 mm “V” central notch was made to nucleate the crack during fatigue test. Four samples were submitted to bending fatigue test to nucleate the cracks and one beam was maintained without cracks to be used as reference. The test was conducted in a controlled way to allow a crack growth visual monitoring to obtain approximated crack length equals to 6.0, 12.0, 18.0 and 24.0 mm. Figure 11b shows the experimental setup.

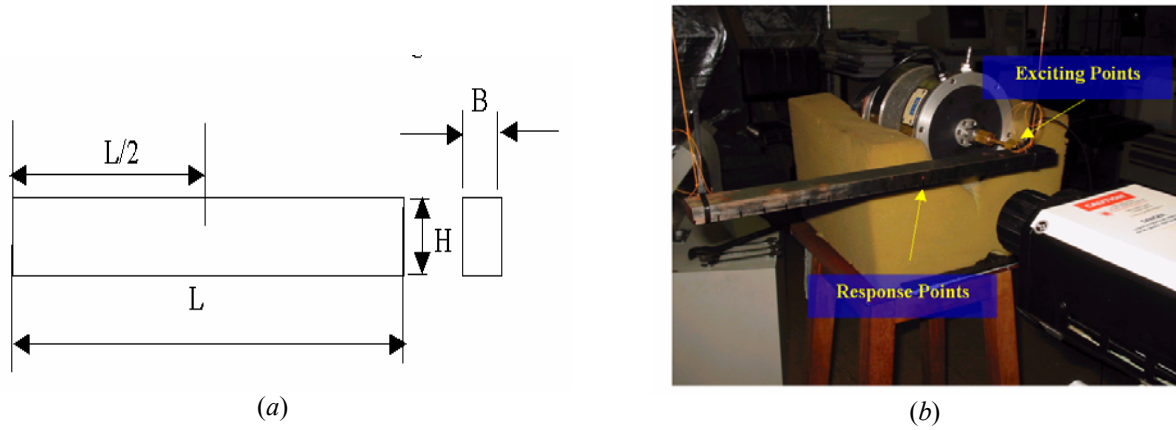


Figure 8. Modal test: (a) main dimensions beam samples; (b) experimental setup.

The modal test was performed in the 5 beams with one excitation and 22 response points. The responses were obtained in velocity (Laser Vibrometer Polytec - OFV303) with a sine sweep excitation force (Force Sensor PCB-482A05) varying the frequency from 100Hz to 10.000Hz in a time interval of 1.6 s. The natural frequencies were identified using the Modal Test module of CAD-X 3.5.e LMS software. Table 1 shows a comparison between experimental and simulated values to the four first natural frequencies results.

The experimental results are compared with simulated numerical results to the beam finite element without ( $\sigma/\sigma_{yp} = 0$ ) and with plasticity effect at crack tip at different stress rates ( $\sigma/\sigma_{yp} = 0.2, 0.4, 0.6$  and  $0.8$ ). These results are shown in Figures 13 - 16 to the first four natural frequencies using plots of relative frequency ( $f_i/f_{ni}$ ) versus relative crack depth ( $a/H$ ).

Table 1. Experimental and numerical frequency results.

Freq [Hz]	Crack Depth [mm]									
	0		6		12		18		24	
	Exp	Num	Exp	Num	Exp	Num	Exp	Num	Exp	Num
1	962,1	967,3	949,4	935,3	856,6	843,1	702,5	666,1	410,2	375,6
2	2594,8	2576,8	2548,8	2573,7	2544,7	2564,5	2527,1	2546,4	2520,1	2511,3
3	4850,6	4830,5	4724,8	4723,9	4414,6	4421,1	3955,3	3903,4	3382,8	3314,9

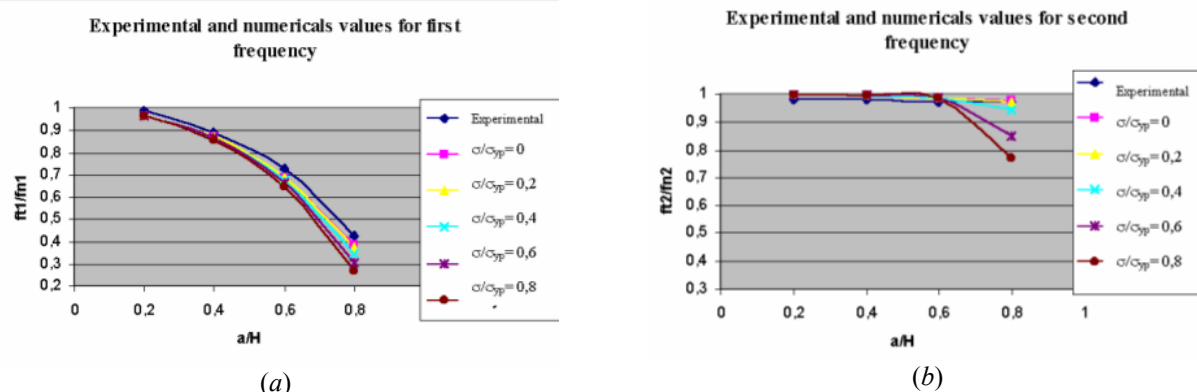


Figure 9. First and second bending natural frequency: experimental and simulated results.

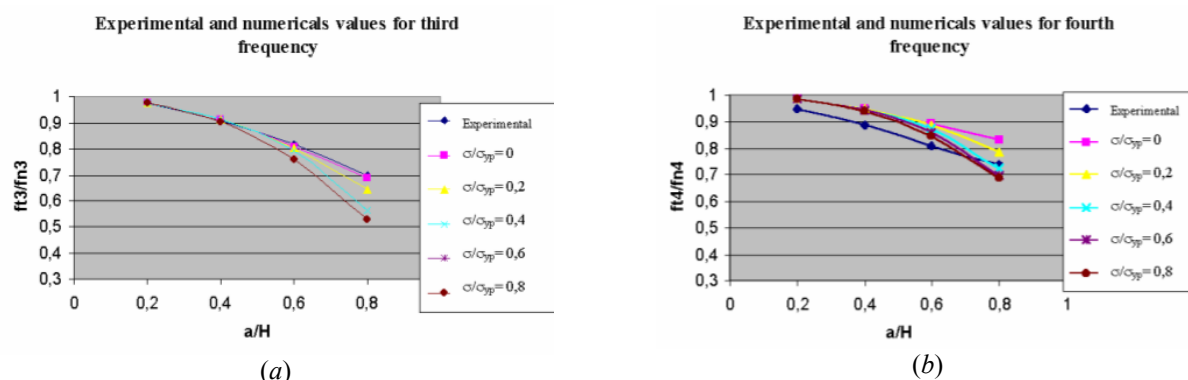


Figure 10. Third and fourth bending natural frequency: experimental and simulated results.

For the three first natural frequencies the experimental and simulated results present a good agreement. However, for the fourth natural frequency there is significant difference between experimental and numerical values. It is believed that this difference comes from the modal analysis frequency identification.

For all cases including the plastic zone effect it was observed that when the rate  $\sigma/\sigma_{yp}$  increase the relative natural frequencies values ( $fti/fni$ ) decrease. This behavior is in agreement with ones obtained by Krawczuk, Zak and Ostachowics (2000).

## 5. Conclusion

A two nodes cracked beam finite element with rectangular cross section, three degrees of freedom per node, and a crack position in the middle of element length was implemented in MATLAB environment. The results of implemented element show a good agreement with the values presented by Qian, Gu & Jiang (1990). For all cases, it was observed the increase of beam flexibility when the crack length increase, which implies in natural frequency reduction.

Experimental modal analysis was performed in five equal dimensions steel beam samples, but with four including different crack depth and one without crack. Experimental natural frequency results were in a good agreement with simulated ones, except to the fourth, which the discrepancy could be due some imprecision on the modal analysis identification. For the cases where the plastic zone was considered, it was verified that the element presents a tendency in reducing the natural frequency values when the rate  $\sigma/\sigma_{yp}$  is increased.

## 6. Acknowledgements

The authors are grateful to the companies SIFCO S/A and LMS International, as well as to the government agencies Fundação de Amparo à Pesquisa do Estado de São Paulo – FAPESP, Conselho Nacional de Desenvolvimento Científico e Tecnológico – CNPq and Fundação CAPES, for the financial support.

## 7. References

- Dimarogonas, A. D.; Papadopoulos, C. A. Vibration of cracked shafts in bending. *Journal of sound and vibration*, v. 91, p. 583-593, Jan. 1983.
- Kisa, M.; Brandon, J.; Topcu, M. Free vibration of cracked beams by a combination of finite elements and component mode synthesis methods. *Computers & Structures*, v. 67, p. 215-223, Jan. 1998.
- Krawczuk, M., Zak, A.; Ostachowicz W. Elastic beam finite element with a transverse elasto-plastic crack. *Finite Elements in Analysis and Design*, v. 34, p. 61-73, 2000.
- Papadopoulos, C. A.; Dimarogonas, A. D. Coupled longitudinal and bending vibrations of a rotating shaft with an open crack. *Journal of sound and vibration*, v. 117, p. 81-93, Jun. 1986.
- Pavanello, R., MefLab: MATLAB Finite Element Code, Unicamp, 1995.
- Qian, G. L.; Gu, S. N.; Jiang, J. S. The dynamic behavior and crack detection of a beam with a crack. *Journal of Sound and Vibration*, v. 138, p. 233-243, 1990.
- Rizzatti, L., *Experimental and numeric dynamic analysis of cracked beam*,: Faculdade de Engenharia Mecânica, Universidade Estadual de Campinas, 2004. 70 p. Dissertação (Mestrado)
- Sekhar, A. S.; Balaji Prasad P. Dynamic analysis of a rotor system considering a slant crack in the shaft. *Journal of Sound and Vibration*, v. 208, p. 457-474, Jul. 1997.
- Sekhar, A. S.; Prabhu, B.S. Vibration and stress fluctuation in cracked shafts. *Journal of Sound and Vibration*, v. 169, p. 655-667, Jul. 1994.
- Tada, H.; Paris, P.C.; Irwin, G.R. The stress analysis of cracks handbook. 3<sup>rd</sup>. ed. New York: The American Society of Mechanical Engineers, 2000, 681p.

## 8. Responsibility notice

The authors are the only responsible for the printed material included in this paper.